EPJ manuscript No.
(will be inserted by the editor)

Nuclear Modification Factor Using Tsallis Non-extensive Statistics

Sushanta Tripathy[1], Trambak Bhattacharyya[2], Prakhar Garg[1,a], Prateek Kumar[1], Raghunath Sahoo[1,b], and Jean Cleymans[2]

[1] Discipline of Physics, School of Basic Sciences, Indian Institute of Technology Indore, Simrol, M.P.- 453552, India
[2] UCT-CERN Research Centre and Department of Physics, University of Cape Town, Rondebosch 7701, South Africa

arXiv:1606.06898v2 [nucl-th] 25 Sep 2016

September 27, 2016

Abstract. The nuclear modification factor is derived using Tsallis non-extensive statistics in relaxation time approximation. The variation of the nuclear modification factor with transverse momentum for different values of the non-extensive parameter, q, is also observed. The experimental data from RHIC and LHC are analysed in the framework of Tsallis non-extensive statistics in a relaxation time approximation. It is shown that the proposed approach explains the R_{AA} of all particles over a wide range of transverse momentum but does not seem to describe the rise in R_{AA} at very high transverse momenta.

PACS. 25.75.-q Relativistic heavy-ion collisions – 25.75.Cj Heavy-quark production in heavy-ion collisions

1 Introduction

One of the major goals of studying heavy-ion collisions at high-energies is to search for a deconfined state of quarks and gluons, also known as quark gluon plasma (QGP), and to study its properties. The bulk properties of the QGP are governed by light quarks and gluons. The heavy quarks act as probes for QGP properties due to the fact that they witness the entire plasma evolution as they are produced in the initial hard scattering and endure until hadronization. Also, as their time scale of thermalization is longer than that of light quarks, they can retain the entire interaction history more effectively. Similarly, the energy loss of light quarks becomes important to study the flavor dependence of the energy loss in heavy-ion collisions.

The energy loss is more for high-p_T heavy and light quark flavors [1,2,3,4] due to interaction with the medium. Finally they appear as constituents of hadrons. The propagation of energetic quarks through the medium has been treated as Brownian motion which is described by means of Fokker-Planck equation. In this equation, the interaction is encoded in drag and diffusion coefficients. Many theoretical efforts have been made using Fokker-Planck equation to reproduce the experimentally observed value of R_{AA} of heavy and light quarks [5,6,7,8,9,10,11,12,13]. Also, there have been studies to elucidate the dominant mode of energy loss [5] or the flavor dependence of energy loss [14,15]. But, till date the issues are far from being settled [16].

The nuclear modification factor (R_{AA}) is a measure of the modification of particle production. It can be represented as

$$R_{AA} = \frac{f_{fin}}{f_{in}}, \tag{1}$$

where f_{in} is the distribution of the highly energetic particles immediately after their formation and f_{fin} is the distribution of the particles after the interaction with the medium.

R_{AA} is defined as

$$R_{AA}(p_T) = \frac{(1/N_{AA}^{evt}) d^2N_{AA}/dydp_T}{(\langle N_{coll}\rangle/\sigma_{NN}^{inel}) \times d^2\sigma_{pp}/dydp_T}, \tag{2}$$

where $d^2N_{AA}/dydp_T$ is the yield in A+A collisions, $\langle N_{coll}\rangle$ is the number of binary nucleon-nucleon collisions averaged over the impact parameter range of the corresponding centrality bin calculated by Glauber Monte-Carlo simulation [17]. σ_{NN}^{inel} is the inelastic cross section and $d^2\sigma_{pp}/dydp_T$ is the differential cross section for inelastic $p+p$ collisions. N_{AA}^{evt} is the number of events in A+A collisions. If, $R_{AA} = 1$, this indicates that A+A collisions are mere superposition of scaled $p+p$ collisions. A deviation of R_{AA} from unity indicates the medium modification. It has been observed that high-p_T particle yields in Au+Au and Pb+Pb collisions at RHIC and LHC are suppressed as compared to $p+p$ collisions [18,19], which suggests the formation of a dense medium.

In this work, we represent the initial distribution of the energetic particles with the help of Tsallis power law

[a] *P*resent Address: Department of Physics and Astronomy, Stony Brook University, SUNY, Stony Brook, NY 11794-3800, USA
[b] *e*-mail: Raghunath.Sahoo@cern.ch (corresponding author)

distribution parameterized by the Tsallis q parameter and the Tsallis temperature T, remembering the fact that their genesis is due to very hard scatterings. We plug the initial distribution (f_{in}) in Boltzmann Transport Equation (BTE) and solve it with the help of Relaxation Time Approximation (RTA) of the collision term to find out the final distribution (f_{fin}). Hence, the ratio in Eq. 1 expressible in terms of q, T and relaxation time τ can be computed and compared with the experimentally observed values.

The paper is organized as follows. In section 2, the nuclear modification factor is derived using RTA of the BTE and the expression for nuclear modification factor is derived. In section 3, fits to the experimental data using the proposed model along with results and discussions are presented; and lastly, we summarize our findings in section 4.

2 Nuclear Modification Factor in Relaxation time approximation (RTA)

The evolution of the particle distribution owing to its interaction with the medium particles can be studied through Boltzmann transport equation,

$$\frac{df(x,p,t)}{dt} = \frac{\partial f}{\partial t} + \boldsymbol{v}.\nabla_x f + \boldsymbol{F}.\nabla_p f = C[f], \tag{3}$$

where $f(x,p,t)$ is the distribution of particles which depends on position, momentum and time. $\mathbf{v}$ is the velocity and $\mathbf{F}$ is the external force. ∇_x and ∇_p are the partial derivatives with respect to position and momentum, respectively. $C[f]$ is the collision term which encodes the interaction of the probe particles with the medium. The Boltzmann Transport Equation has earlier also been used in relaxation time approximation to study the time evolution of temperature fluctuation in a non-equilibrated system [20].

Assuming homogeneity of the system ($\nabla_x f = 0$) and absence of external force ($F = 0$), the second and third terms of the above equation become zero and Eq. 3 becomes,

$$\frac{df(x,p,t)}{dt} = \frac{\partial f}{\partial t} = C[f] \tag{4}$$

In relaxation time approximation [21,22], the collision term can be expressed as,

$$C[f] = -\frac{f - f_{eq}}{\tau} \tag{5}$$

where f_{eq} is Boltzmann local equilibrium distribution characterized by a temperature T_{eq}. τ is the relaxation time, the time taken by a non-equilibrium system to reach equilibrium. With the ansatz in Eq. 5, Eq. 4 becomes,

$$\frac{\partial f}{\partial t} = -\frac{f - f_{eq}}{\tau} \tag{6}$$

Solving the above equation in view of initial conditions i.e. at $t = 0, f = f_{in}$ and at $t = t_f, f = f_{fin}$; leads to,

$$f_{fin} = f_{eq} + (f_{in} - f_{eq})e^{-\frac{t_f}{\tau}}, \tag{7}$$

where t_f is the freeze-out time. Using Eq.7, the nuclear modification factor can be expressed as,

$$R_{AA} = \frac{f_{fin}}{f_{in}} = \frac{f_{eq}}{f_{in}} + \left(1 - \frac{f_{eq}}{f_{in}}\right) e^{\frac{-t_f}{\tau}} \tag{8}$$

Eq. 8 is the derived nuclear modification factor after incorporating relaxation time approximation, which is the basis of our analysis in the present paper. It involves the (power law-like) initial distribution and the equilibrium distribution. In this analysis, the initial distribution is parameterized using the thermodynamically consistent Tsallis distribution [23].

Tsallis statistics is widely used to analyse the detected particle spectra in high-energy collisions starting from e^+e^-, $p+p$ to heavy-ions [24,25,26,27,28,29,30,31,32,33,34,35, 36,37,38,39,40,41]. Also, as the system stays away from thermal equilibrium during the formation of highly energetic particles immediately after the collision, the particle distribution can be parameterized with the help of Tsallis distribution. A thermodynamically consistent non-extensive Tsallis distribution function, to be used as the initial distribution, is given by, [23]

$$f_{in} = \frac{gV}{(2\pi)^2} p_T m_T \left[1 + (q-1)\frac{m_T}{T}\right]^{-\frac{q}{q-1}}, \tag{9}$$

which is used for studying the particle distribution stemming from the proton-proton collisions as discussed in Ref. [23].

The Boltzmann equilibrium distribution is given by

$$f_{eq} = \frac{gV}{(2\pi)^2} p_T m_T e^{-\frac{m_T}{T_{eq}}} \tag{10}$$

Here, V is the system volume, $m_{\rm T} = \sqrt{p_T^2 + m^2}$ is the transverse mass and q is the non-extensive parameter, which measures the degree of deviation from equilibrium. Using Eqs. 9 and 10 (both for mid-rapidity and for zero chemical potential) nuclear modification factor can be expressed as,

$$R_{AA} = \frac{e^{-\frac{m_T}{T_{eq}}}}{(1 + (q-1)\frac{m_T}{T})^{-\frac{q}{q-1}}} + \left[1 - \frac{e^{-\frac{m_T}{T_{eq}}}}{(1 + (q-1)\frac{m_T}{T})^{-\frac{q}{q-1}}}\right] e^{-\frac{t_f}{\tau}} \tag{11}$$

This will be compared to experimental results in the next section.

3 Results and Discussion

To illustrate the formula given in Eq. 11 we take as an example the case of the J/ψ particle. The variation of nuclear modification factor with transverse momentum for

different values of non-extensive parameter is plotted in Fig. 1. For this figure, $m = 3.096$ GeV, $T_{eq} = 0.16$ GeV, $T = 0.17$ GeV and $t_f/\tau = 1.06$ are taken. It is observed that for higher values of q, R_{AA} decreases for all the values of p_T. This suggests that when the initial distribution remains closer to equilibrium, the suppression becomes less. The model presented here fails to describe the increase in R_{AA} at larger transverse momenta, which is seen in experimental data for light flavor hadrons.

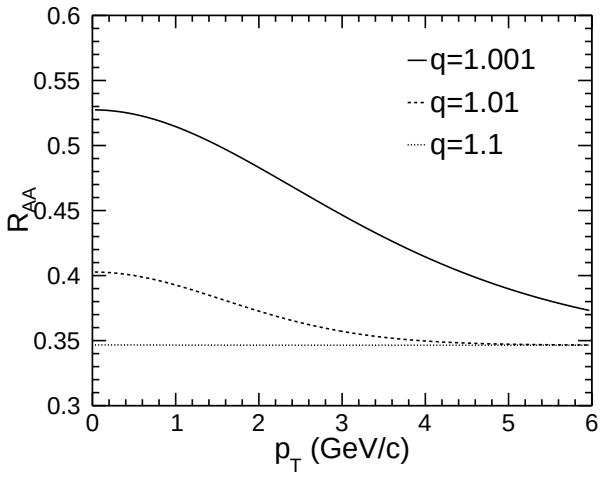

Fig. 1: Nuclear modification factor versus p_T for different values of the non-extensive parameter using Tsallis Boltzmann distribution as shown in Eq.11. Here $m = 3.096$ GeV, $T_{eq} = 0.16$ GeV, $T = 0.17$ GeV and $t_f/\tau = 1.06$.

We now proceed to the more detailed analysis of the experimental data with the model proposed above. Keeping all the parameters free, we fit the spectra for different particles in different centralities for Pb+Pb and Au+Au collisions using TMinuit class available in ROOT library [42] to get a convergent solution. The convergent solution is obtained by χ^2 minimization technique. Here T, q and t_f/τ are the fitting parameters for the experimental data. The equilibrium temperature T_{eq} is fixed to 160 MeV throughout the analysis.

In our analysis, it is observed that the fitting of low p_T for light flavor particles fails due to the reason that it involves different physical processes such as regeneration, coalescence, shadowing etc., which are out for the scope of present formalism. But in heavy flavor particles, no such processes are involved at the discussed energies. Thus our proposed model explains successfully the heavy flavor R_{AA} data. Also, for very high-p_T, our model fails to explain the increase in R_{AA} (most prominent for $K^{\pm}$ in Fig. 3).

Fig. 2 shows the fitting of experimental data using Eq.11 for π^0 meson in most central Au+Au collisions at $\sqrt{s_{NN}}$= 200 GeV. The derived expression for R_{AA} fits the data in intermediate to high-p_T range. Also, in Fig. 2 we show the fitting of experimental data for $\pi^+ + \pi^-$ in most central Pb+Pb collisions at $\sqrt{s_{NN}}$= 2.76 TeV. The model considered here, fits the data from intermediate to high-p_T range. The fitting parameters are shown in table 1 along with the χ^2/ndf values.

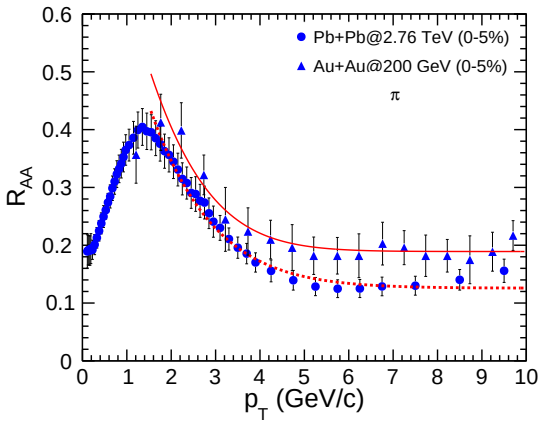

Fig. 2: (Color Online) Fitting of experimental data for nuclear modification factor with our proposed model (Eq.11) for π^0[43] (blue triangles) in Au+Au collisions at $\sqrt{s_{NN}}$= 200 GeV and $\pi^+ + \pi^-$[44] in Pb+Pb collisions at $\sqrt{s_{NN}}$= 2.76 TeV (blue dots). The solid red line shows the fitting for blue triangles and the dotted red line shows the fitting for blue dots.

Similarly, in Fig. 3 we fit the experimental data for $K^+ + K^-$ in most central Pb+Pb collisions at $\sqrt{s_{NN}}$= 2.76 TeV. The proposed model fits the data for intermediate p_T range. The derived expression of R_{AA} could not fit the data in high-p_T range as an enhancement is observed in high-p_T. The fitting parameters are shown table 1 along with the χ^2/ndf values.

Fig. 4 shows the fitting of experimental data for K^0_S in most central Pb+Pb collisions at $\sqrt{s_{NN}}$= 2.76 TeV. The proposed model fits the data for intermediate to high-p_T range. The fitting parameters are shown table 1 along with the χ^2/ndf values.

Fig.5 shows the fitting of experimental data for $p+\bar{p}$ in most central Pb+Pb collisions at $\sqrt{s_{NN}}$= 2.76 TeV. The proposed model fits the data for intermediate to high-p_T range. χ^2/ndf value and the fitting parameters are shown table 1.

Fig. 6 shows the fitting of experimental data using Eq.11 for $\Lambda + \bar{\Lambda}$ in most central Pb+Pb collisions at $\sqrt{s_{NN}}$= 2.76 TeV. The proposed model fits the data from intermediate to high-p_T range starting from 2 GeV to 14 GeV. χ^2/ndf value and the fitting parameters are shown table 1.

In Fig. 7 we fit the experimental data for D^0 meson in most central, (0-10)% Au+Au collisions at $\sqrt{s_{NN}}$= 200 GeV. As less data points are available, the fitting parameters cannot be established very well. Thus the χ^2/ndf value is very high compared to other particles, which can

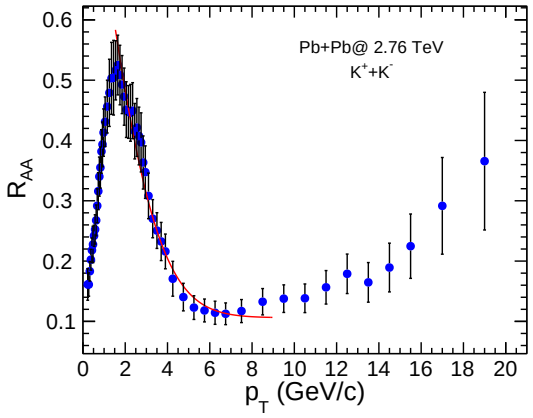

Fig. 3: (Color Online) Fitting of experimental data for nuclear modification factor with our proposed model(Eq.11) for $K^+ + K^-$[44] in most central Pb+Pb collisions at $\sqrt{s_{NN}}$= 2.76 TeV (blue dots). The solid red line shows the fitting for blue dots.

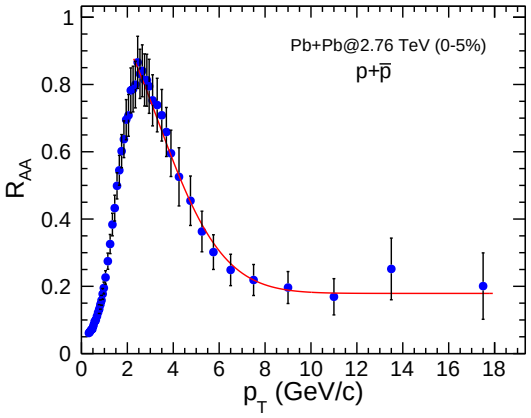

Fig. 5: (Color Online) Fitting of experimental data for nuclear modification factor with our proposed model (Eq.11) for $p+\bar{p}$ [44] in most central Pb+Pb collisions at $\sqrt{s_{NN}}$= 2.76 TeV (blue dots). The solid red line shows the fitting for blue dots.

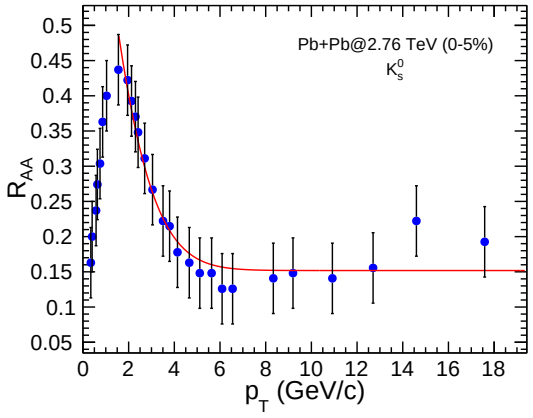

Fig. 4: (Color Online) Fitting of experimental data for nuclear modification factor with our proposed model (Eq.11) for K^0_S in most central Pb+Pb collisions at $\sqrt{s_{NN}}$= 2.76 TeV(blue dots). The solid red line shows the fitting for blue dots.

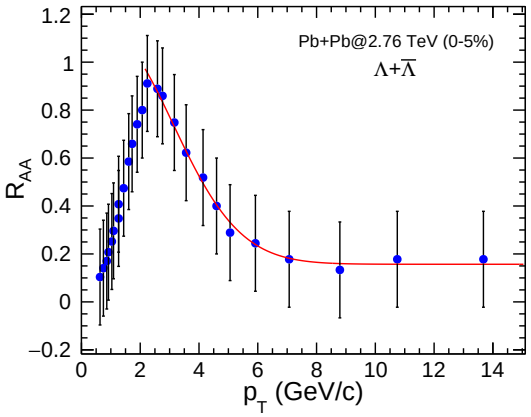

Fig. 6: (Color Online) Fitting of experimental data for nuclear modification factor with our proposed model (Eq.11) for $\Lambda+\bar{\Lambda}$ in most central Pb+Pb collisions at $\sqrt{s_{NN}}$= 2.76 TeV (blue dots). The solid red line shows the fitting for blue dots.

be seen table 1. Also in Fig. 7 we show the fitting of experimental data for D^0 meson for (30-50)% central Pb+Pb collisions at $\sqrt{s_{NN}}$= 2.76 TeV. The proposed model fits the data accurately for all the p_T ranges as the enhancement is not involved which originate from regeneration through coalescence mechanism. χ^2/ndf value and the fitting parameters are shown table 1.

In Fig. 8 we show the fitting of experimental data for J/ψ in minimum bias Pb+Pb collisions (0-90% centrality) at $\sqrt{s_{NN}}$= 2.76 TeV. The proposed model fits the data accurately for all p_T ranges as the enhancement in R_{AA} is not observed in experimental J/ψ data. The χ^2/ndf value and the fitting parameters are shown table 1. We have explicitly checked that the proposed model also explains the J/ψ R_{AA} for central Pb+Pb collisions at $\sqrt{s_{NN}}$= 5.02 TeV.

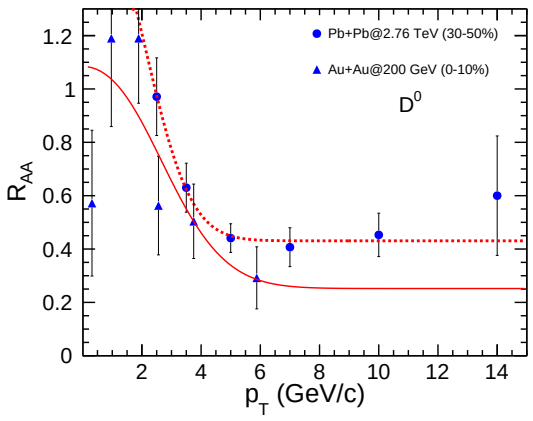

Fig. 7: (Color Online) Fitting of experimental data for nuclear modification factor with our proposed model (Eq.11) for D^0 meson [45] (blue triangles) in most central Au+Au collisions at $\sqrt{s_{NN}}$= 200 GeV and D^0 meson [46] in (30-50)% central Pb+Pb collisions at $\sqrt{s_{NN}}$= 2.76 TeV (blue dots). The solid red line shows the fitting for blue triangles and the dotted red line shows the fitting for blue dots.

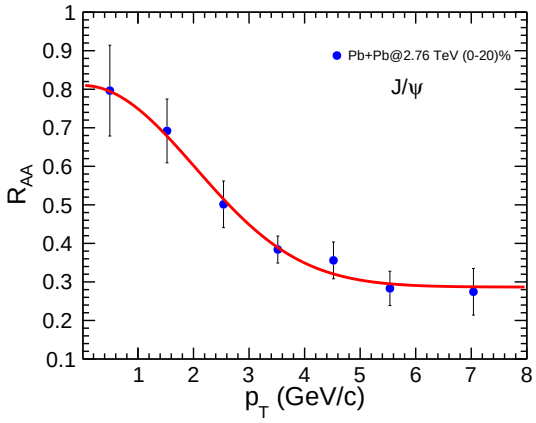

Fig. 8: (Color Online) Fitting of experimental data for nuclear modification factor with our proposed model (Eq.11) for J/ψ [47] in Pb+Pb collisions at $\sqrt{s_{NN}}$= 2.76 TeV (blue dots) with centrality (0-90)%. The solid red line shows the fitting to experimental data.

Finally, we have shown the variation of t_f/τ with mass in Fig. 9. It is observed that t_f/τ decreases with increasing the particle mass, which suggests that the heavy particles have more relaxation time compared to lighter particles. Note here, that t_f is the freeze-out time, and τ is the relaxation time, which differs from particle to particle, as the equilibration depends on the particle species and their interaction with the rest of the medium. Intuitively, the heavier the particle is, the more is the relaxation time. And hence, t_f/τ becomes less and the degrees of freedom are shared with other parameters used in the fit.

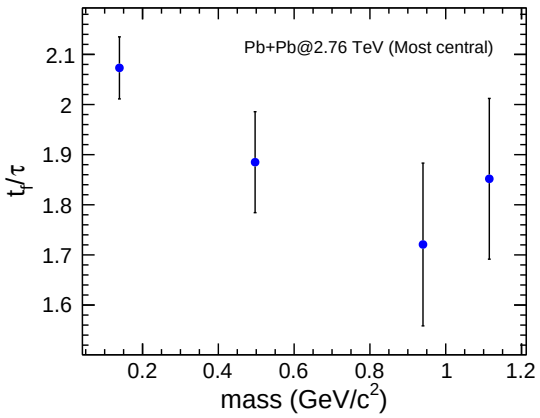

Fig. 9: (Color Online) t_f/τ as a function of particle mass for most central Pb+Pb collisions at $\sqrt{s_{NN}}$= 2.76 TeV.

4 Summary and Conclusion

In this work, we represent the initial distribution of the energetic particles with the help of Tsallis power law distribution parameterized by the Tsallis q parameter and the Tsallis temperature T, remembering the fact that their genesis is due to very hard scatterings. We plug the initial distribution (f_{in}) in Boltzmann Transport Equation (BTE) and solve it with the help of Relaxation Time Approximation (RTA) of the collision term to find out the final distribution (f_{fin}). Hence, the ratio in Eq. 1 expressible in terms of q, T and relaxation time, τ can be computed and compared with the experimentally observed values. The variation of nuclear modification factor with transverse momentum for different values of non-extensive parameter, is also observed. The suppression is found to be higher for a system with higher degree of deviation from equilibrium. Also, we analyse the experimental data from RHIC and LHC with calculated nuclear modification factor. It is observed that the calculated R_{AA} explains accurately for heavy flavor particles in all p_T range, but it can only explain R_{AA} for light flavor particles in intermediate to high-p_T range with an exception for kaons, where the enhancement at high-p_T can not be explained with the present model. The relaxation time, as found from data, is higher for heavy particles.

Acknowledgements

ST acknowledges the financial support by DST INSPIRE program of Govt. of India. TB acknowledges the discussion with Dr. Santosh K. Das.

Table 1: Centrality, χ^2/ndf and different extracted parameters after fitting Eq. 11 to the R_{AA} data of different particles for Pb+Pb collisions and Au+Au collisions at $\sqrt{s_{NN}}$= 2.76 TeV and $\sqrt{s_{NN}}$= 200 GeV, respectively.

Pb+Pb 2.76 TeV					
Particle	Centrality(%)	χ^2/ndf	t_f/τ	q	T (GeV)
$\pi^+ + \pi^-$	0-5	0.364461	2.07313 ± 0.061906	1.00151 ± 0.00149	0.17854 ± 0.00143
$K^+ + K^-$	0-5	0.390686	2.24302 ± 0.098624	1.00406 ± 0.00125	0.16803 ± 0.00133
K_s^0	0-5	0.284477	1.88499 ± 0.100713	1.00410 ± 0.00373	0.17320 ± 0.00379
$p + \bar{p}$	0-5	0.267087	1.72079 ± 0.163273	1.00378 ± 0.00079	0.15771 ± 0.00111
$\Lambda + \bar{\Lambda}$	0-5	0.017809	1.85201 ± 0.649860	1.00600 ± 0.00369	0.15411 ± 0.00512
D^0	30-50	0.262131	0.84223 ± 0.099520	1.01915 ± 0.01202	0.13538 ± 0.01568
J/ψ	0-90	0.155083	1.06248 ± 0.157049	1.01252 ± 0.00998	0.14676 ± 0.01408
Au+Au 200 GeV					
π^0	0-5	0.24223	1.66530 ± 0.05601	1.0050 ± 0.00525	0.17483 ± 0.00550
D^0	0-10	2.27963	1.37833 ± 0.63285	1.0076 ± 0.00594	0.15273 ± 0.00688

References

1. I. Arsene *et al.* [BRAHMS Collaboration], Phys. Lett. B **650**, 219 (2007).
2. J. D. Bjorken, Phys. Rev. D **27**, 140 (1983).
3. M. Pluemer, M. Gyulassy and X. N. Wang, Nucl. Phys. A **590**, 511C (1995).
4. R. Baier, Y. L. Dokshitzer, S. Peigne and D. Schiff, Phys. Lett. B **345**, 277 (1995).
5. J. e. Alam, P. Roy and A. K. Dutt-Mazumder, arXiv: hep-ph/0604131.
6. B. Svetitsky, Phys. Rev. D **37**, 2484 (1988).
7. M. Golam Mustafa, D. Pal and D. K. Srivastava, Phys. Rev. C **57**, 889 (1998) 3499(E) (1998).
8. H. van Hees, V. Greco and R. Rapp, Phys. Rev. C **73**, 034913 (2006).
9. H. van Hees, M. Mannarelli, V. Greco and R. Rapp, Phys. Rev. Lett. **100**, 192301 (2008).
10. S. K. Das, J. e. Alam and P. Mohanty, Phys. Rev. C **80**, 054916 (2009).
11. S. K. Das, F. Scardina, S. Plumari and V. Greco, Phys. Lett. B **747**, 260 (2015).
12. W. M. Alberico, *et al.*, Eur. Phys. J. C **73**, 2481 (2013).
13. S. Mazumder, T. Bhattacharyya, J. e. Alam and S. K. Das, Phys. Rev. C **84**, 044901 (2011).
14. B. G. Zakharov, JETP Lett. **96**, 616 (2013).
15. B. Z. Kopeliovich, I. K. Potashnikova and I. Schmidt, Phys. Rev. C **82**, 037901 (2010).
16. I. Kolbe and W. A. Horowitz, arXiv:1511.09313 [hep-ph].
17. R. J. Glauber and G. Matthiae, Nucl. Phys. B **21**, 135 (1970).
18. S. S. Adler *et al.* (PHENIX Collaboration), Phys. Rev. Lett. **91**, 072301 (2003).
19. K. Aamodt *et al.* (ALICE Collaboration), Phys. Lett. B **696**, 30 (2011).
20. T. Bhattacharyya, P.Garg, R. Sahoo, P. Samantray, Eur. Phys. J. A **52**, 283 (2016).
21. R. Balescu, *Equilibrium and Non-Equilibrium Statistical Mechanics*, John Wiley and Sons, USA (1975).
22. W. Florkowski and R. Ryblewski, Phys. Rev. C **93**, 064903 (2016)
23. J. Cleymans, D. Worku, J. Phys. G **39**, 025006 (2012).
24. D. Thakur, S. Tripathy, P. Garg, R. Sahoo and J. Cleymans, arXiv:1601.05223 [hep-ph].
25. I. Bediaga, E.M.F. Curado, J.M. de Miranda, Physica A **286**, 156 (2000).
26. G. Wilk and Z. Włodarczyk, Acta Phys. Polon. B **46**, 1103 (2015).
27. K. Ürmössy, G.G. Barnaföldi, T.S. Biró, Phys. Lett. B **701**, 111 (2011).
28. K. Ürmössy, G.G. Barnaföldi, T.S. Biró, Phys. Lett. B **718**, 125 (2012).
29. P. K. Khandai, P. Sett, P. Shukla, V. Singh, Int. Jour. Mod. Phys. A **28**, 1350066 (2013).
30. B.-C. Li, Y.-Z. Wang and F.-H. Liu, Phys. Lett. B **725**, 352 (2013).
31. L. Marques, J. Cleymans and A. Deppman Phys. Rev. D **91**, 054025 (2015).
32. B. I. Abelev *et al.* (STAR collaboration), Phys. Rev. C **75**, 064901 (2007).
33. A. Adare *et al.* (PHENIX collaboration), Phys. Rev. D **83**, 052004 (2011).
34. A. Adare *et al.* (PHENIX collaboration), Phys. Rev. C **83**, 064903 (2011).
35. K. Aamodt *et al.* (ALICE collaboration), Phys. Lett. B **693**, 53 (2010).
36. K. Aamodt *et al.* (ALICE collaboration), Eur. Phys. J C **71**, 1655 (2011).
37. V. Khachatryan *et al.* (CMS collaboration), J. of High Eng. Phys. **02**, 041 (2010).
38. V. Khachatryan *et al.* (CMS collaboration), Phys. Rev. Lett. **105**, 022002 (2010).
39. G. Aad, et al. (ATLAS collaboration), New J. Phys. **13**, 053033 (2011).
40. B. Abelev *et al.* (ALICE collaboration), Phys. Rev. Letts. **109**, 252301 (2012).
41. T. Bhattacharyya, J. Cleymans, A. Khuntia, P. Pareek and R. Sahoo, Eur. Phys. J. A **52**, 30 (2016).
42. CERN ROOT V.5.34/32 (June 23, 2015) Package: http://root.cern.ch.
43. A. Adare *et al.* (PHENIX Collaboration), Phys. Rev. Lett. **101**, 232301 (2008).
44. B. B. Abelev *et al.* (ALICE Collaboration), Phys. Lett. B **736**, 196 (2014).
45. L. Adamczyk *et al.* (STAR Collaboration), Phys. Rev. Lett. **113**, 142301 (2014).
46. B. B. Abelev *et al.* (ALICE Collaboration), Phys. Rev. C **90**, 034904 (2014).
47. B. B. Abelev *et al.* (ALICE Collaboration), Phys. Lett. B **734**, 314 (2014).